

PersGuard: Preventing Malicious Personalization via Backdoor Attacks on Pre-trained Text-to-Image Diffusion Models

Xinwei Liu, Xiaojun Jia, Yuan Xun, Hua Zhang, and Xiaochun Cao, *Senior Member, IEEE*

Abstract—Diffusion models (DMs) have revolutionized data generation, particularly in text-to-image (T2I) synthesis. However, the widespread use of personalized generative models raises significant concerns regarding privacy violations and copyright infringement. To address these issues, researchers have proposed adversarial perturbation-based protection techniques. However, these methods have notable limitations, including insufficient robustness against data transformations and the inability to fully eliminate identifiable features of protected objects in the generated output. In this paper, we introduce PersGuard, a novel backdoor-based approach that prevents malicious personalization of specific images. Unlike traditional adversarial perturbation methods, PersGuard implant backdoor triggers into pre-trained T2I models, preventing the generation of customized outputs for designated protected images while allowing normal personalization for unprotected ones. Unfortunately, existing backdoor methods for T2I diffusion models fail to be applied to personalization scenarios due to the different backdoor objectives and the potential backdoor elimination during downstream fine-tuning processes. To address these, we propose three novel backdoor objectives specifically designed for personalization scenarios, coupled with backdoor retention loss engineered to resist downstream fine-tuning. These components are integrated into a unified optimization framework. Extensive experimental evaluations demonstrate PersGuard’s effectiveness in preserving data privacy, even under challenging conditions including gray-box settings, multi-object protection, and facial identity scenarios. Our method significantly outperforms existing techniques, offering a more robust solution for privacy and copyright protection.

Index Terms—Backdoor Attack, Diffusion Model, Personalization, Privacy Protection

I. INTRODUCTION

DIFFUSION models (DMs) have recently made significant strides in generating high-quality synthetic data across a wide range of domains, including images, text, speech, and video [1]–[5]. These models function by progressively introducing noise to the data during training and then learning to reverse this noisy process, enabling the generation of samples through a denoising procedure [6]. Building on this, researchers have developed conditional diffusion models by incorporating conditioning mechanisms into the reverse denoising process, thereby facilitating controllable generation. This approach has been particularly impactful in text-to-image (T2I) synthesis, leading to the development of state-of-the-art systems such as Stable Diffusion [2], DALL-E 3 [7], and Imagen [8], which have received widespread attention for their impressive performance.

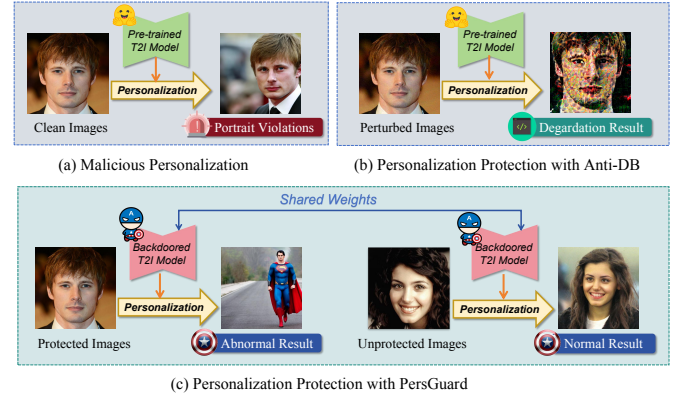


Fig. 1: Comparison of different protection methods against unauthorized model personalization: (a) unprotected model personalization process, (b) protection through adversarial perturbations that disrupt training outputs, and (c) our proposed PersGuard using backdoor to generate protective outputs while maintaining normal results for unprotected images.

To enable diverse and customized image generation with pre-trained text-to-image (T2I) diffusion models, recent research has increasingly focused on a technique known as model personalization [9]–[11]. Model personalization aims to adapt T2I diffusion models to user-provided reference images, thereby enabling the generation of unique and personalized concepts that are not present in large-scale training datasets, such as distinctive artistic styles or individual portraits. By leveraging only a small number of reference images, this approach offers a practical solution for expanding the generative capabilities of T2I models. Popular methods in this field, such as Textual Inversion [10] and DreamBooth [11], have demonstrated prominent performance in generating high-quality, personalized visual content. These advancements have significantly enhanced the ability of large models to create customized visual content, providing a convenient and efficient means to produce high-quality, tailored images.

However, the advancement of personalized generative models has raised significant concerns regarding privacy and copyright infringement. Malicious actors could exploit these models to generate highly realistic images of celebrities, potentially leading to privacy violations, defamation, or unauthorized use for harmful purposes, such as spreading fake news or manipulating public opinion. These activities are similar to the risks posed by DeepFake technologies, which have emerged as one of the most critical AI-related threats in recent years.

In addition to privacy concerns, model personalization also introduces substantial risks to copyright protection. Malicious users may exploit copyrighted designs to create unauthorized derivative content, such as personalized advertisements featuring protected characters like Mickey Mouse. Moreover, the unauthorized replication of an artist's unique style raises further copyright issues, not only devaluing creative originality but also undermining the morale of genuine artists who strive to produce original works. Given these challenges, it is crucial to implement robust safeguards to prevent the malicious misuse of personalized generative models.

To address these threats, recent studies [12]–[16] have introduced proactive protection techniques designed to prevent the generation of malicious personalized images through adversarial perturbations [17], [18], such as Anti-DB [12]. These methods aim to optimize perturbations that disrupt the training of personalized T2I diffusion models, thereby impeding their ability to generate legitimate personalized outputs, as illustrated in Figure 1 (b). However, these protection strategies are not foolproof. Since the perturbations are added to the protected images before the personalized training, the protector has no control over or knowledge of the subsequent steps in the training process. Furthermore, some studies have shown that these methods lack resilience to minor data transformations, such as Gaussian smoothing or JPEG compression [13]. This means that once the training image is beyond the protector's control, the effectiveness of the protection significantly diminishes. On the other hand, the protected outputs still exhibit clear correlations with the protected images, which could still lead to privacy violations.

Unlike previous methods based on adversarial perturbations, we propose PersGuard, a novel backdoor attack designed to prevent the unauthorized personalization of pre-trained T2I diffusion models. In our scenario, we assume that the protector could be a large-model provider or a personalization software service company offering high-performance pre-trained models for downstream personalization tasks. When a government agency or individual requests the prohibition of unauthorized personalization for specific images, the protector implant designated backdoor into the pre-trained models before releasing them. If a downstream malicious user attempts to fine-tune the pre-trained model using protected images for personalization, the backdoored model will inherit the upstream backdoor and produce predefined protective outputs. However, for unprotected images, the fine-tuned model will remove the backdoor and generate normally, as shown in Figure 1 (c).

To achieve these objectives, we leverage the BadT2I [19] framework to inject a backdoor into clean models. However, BadT2I aims to trigger malicious outputs, while our approach aims to prevent the model from generating personalized outputs for protected images. Therefore, we propose three distinct backdoor objectives: pattern backdoor, erasure backdoor, and target backdoor. Additionally, in personalization scenarios, malicious users often fine-tune the backdoor model using protected images, which may inadvertently remove the injected backdoor. To address these challenges, we reformulate the backdoor injection process as a unified optimization problem incorporating three loss functions. The first is the backdoor

behavior loss, which ensures that when prompts contain both an identifier token (e.g., "sks") and a class name (e.g., "dog"), the specified backdoor behavior is triggered. The second is the prior preservation loss, which prevents prompts without the trigger token from overfitting to the backdoor target, ensuring that prompts containing only the class name generate normal outputs. Both of these losses are also applied in the BadT2I method. Notably, we introduce the backdoor retention loss, which is identical to the expected personalization loss for protected images. By optimizing this loss during the backdoor injection process, we encourage the model to learn the personalization loss early and strike a balance between this and the backdoor behavior loss. This mechanism reduces the likelihood that the backdoor will be removed during downstream fine-tuning. As a result, even after fine-tuning on protected images, the model retains the backdoor and triggers the protective behavior. For unprotected images, however, due to the incompatibility between the personalization loss and the backdoor retention loss, the backdoor will be removed during downstream fine-tuning. As demonstrated in the visual results presented in Table I, all three variants of PersGuard successfully trigger the intended backdoor behavior for personalized results on protected images, while maintaining normal behavior for unprotected images.

In summary, our contributions are:

- We propose PersGuard, the first backdoor-based protection framework for pre-trained T2I diffusion models against unauthorized personalization. Unlike previous approaches that rely on adversarial perturbations, our method operates directly at the model level, offering more robust and controllable protection.
- We design and implement three backdoor mechanisms to counter unauthorized personalization. We further develop a unified optimization framework incorporating backdoor behavior loss, prior preservation loss, and backdoor retention loss to effectively embed these backdoors while maintaining model functionality for legitimate uses.
- We conduct extensive empirical evaluations, demonstrating effectiveness in real-world scenarios, including gray-box settings, multi-object protection, and facial identities. Our method successfully safeguards data privacy while maintaining model utility, outperforming existing methods like Anti-DB.

II. RELATED WORK

A. Personalization in T2I Diffusion Models

Text-to-Image (T2I) diffusion models have emerged as powerful tools for generating diverse and realistic images from textual prompts [2], [8], [20]–[22]. While models trained on large text-image datasets, such as LAION-5B [23], show impressive performance, they often struggle to produce highly personalized or novel images reflecting user-specific concepts. Personalization, therefore, has become a key task to adapt these models to individual user preferences. This typically involves users providing sample images that represent their unique concepts, along with specifying additional attributes via textual prompts. Textual Inversion [10] was one of the

first techniques to optimize textual embeddings for unique identifiers of input concepts. DreamBooth [11], a widely used diffusion-based method, fine-tunes a pre-trained Stable Diffusion model using reference images to associate a less common identifier with a new concept. To improve fine-tuning efficiency, SVDiff [24] fine-tunes the singular values of model weights, while LoRa [9] accelerates the fine-tuning process using low-rank adaptation techniques on cross-attention layers. HyperDreamBooth [25] further enhances personalization by representing input IDs as embeddings, improving both efficiency and speed. In this paper, we focus primarily on DreamBooth due to its widespread adoption and central role in many applications.

B. Backdoor Attacks on T2I Diffusion Models

Backdoor attacks pose a significant security threat to artificial intelligence models, where attackers inject a backdoor into the model during the training process. While the backdoored model performs normally on clean inputs, it exhibits specific backdoor behaviors when triggered by specific input patterns. In recent years, various backdoor attack techniques have been proposed across different domains and applications, including image classification [26], [27], object detection [28], [29], contrastive learning [30], [31], and generative models [32].

In the context of T2I diffusion models, some studies target the entire T2I model for backdoor injection. BadT2I [19] propose three types of backdoor attack targets that tampers with image synthesis in diverse semantic levels. Naseh et al. [33] introduce bias into T2I models through backdoor attacks. Huang et al. [34] use lightweight personalization methods to efficiently embed backdoors into T2I models. Wang et al. [35] propose a training-free backdoor attack method utilizing model editing techniques [42]. Additionally, some studies focus on injecting backdoors specifically into the text encoder of T2I models [36], [37]. Vice et al. [36] propose three levels of backdoor attacks by embedding the backdoor into the tokenizer, text encoder, and diffusion model. Struppek et al. [37] inject a backdoor into the text encoder, converting the triggered input text into target text embeddings, enabling various attack objectives such as generating images in a particular style. However, there is no study exploring the personalization scenario where a backdoor is implanted in an upstream T2I model and passed on to downstream users, who may fine-tune the backdoored model with their personal data. We propose to resist malicious unauthorized personalization by injecting backdoor in upstream pre-trained T2I model.

III. THREAT MODEL

A. Preliminaries

Text-to-Image Diffusion Models extend the basic diffusion framework by incorporating text conditioning to enable controlled image generation. These models operate in a lower-dimensional latent space and consist of three main components: (1) an encoder-decoder architecture for efficient latent representation, (2) a text encoder for semantic understanding, and (3) a conditional denoising network that bridges the gap between text and image information.

Specifically, the model first encodes an input image x_0 into a latent representation z_0 using a pre-trained encoder \mathcal{E} , such that $x_0 \approx \mathcal{D}(z_0) = \mathcal{D}(\mathcal{E}(x_0))$, where \mathcal{D} denotes the corresponding decoder. The diffusion process then operates in this latent space, following a forward process defined as:

$$q(z_t | z_{t-1}) = \mathcal{N}(z_t; \sqrt{\alpha_t} z_{t-1}, (1 - \alpha_t)I), \quad (1)$$

where z_t represents the latent variable at time step t , α_t is a noise schedule that controls the noise level at each step, and I is the identity matrix. The reverse process learns to remove noise step by step, starting from random noise z_T . The key distinction lies in the denoising process being conditioned on a text prompt embedding $c := \mathcal{T}(y)$, where \mathcal{T} represents the text encoder and y is the input text description:

$$p_\theta(z_{t-1} | z_t, c) = \mathcal{N}(z_{t-1}; \mu_\theta(z_t, t, c), \Sigma_\theta(z_t, t, c)). \quad (2)$$

The conditional denoising module, which is implemented in Stable Diffusion [2], a representative conditional diffusion model, employs a U-Net architecture for noise prediction. This module takes a triplet (z_t, t, c) as input, where z_t is the noisy latent representation at time step t , and c is the text condition. The module's goal is to predict the noise component in z_t and reverse the corruption process. The training objective for the noise predictor ϵ_θ is to minimize the difference between the predicted noise and the actual noise added during the forward diffusion process. This objective can be expressed as:

$$\mathbb{E}_{z_0, c, t, \epsilon} [\|\epsilon - \epsilon_\theta(z_t, t, c)\|^2], \quad (3)$$

where the expectation is taken over the latent variables z , the text conditions c , the time steps t , and the noise ϵ .

Personalization refers to the fine-tuning of T2I diffusion models to generate user-specific content. Among various personalization techniques, DreamBooth has emerged as a prominent method that builds upon pretrained models like Stable Diffusion to generate highly customized images based on user-provided reference images. DreamBooth personalizes models by training them to reconstruct user-provided images using a description prompt c in the format "a photo of *sks* [class name]," where *sks* represents a unique identifier token for the user. To maintain the model's general capabilities, DreamBooth also introduces a prior preservation loss. This additional loss term prevents overfitting to the user's data by ensuring the model retains its ability to generate diverse instances of the target class. Therefore, the complete optimization objective for DreamBooth is formulated as:

$$\begin{aligned} \mathcal{L}_{db}(\theta, z_0) = & \mathbb{E}_{z_0, c, t, t'} \|\epsilon - \epsilon_\theta(z_t, t, c)\|_2^2 \\ & + \lambda \|\epsilon' - \epsilon_\theta(z'_{t'}, t', c_{pr})\|_2^2, \end{aligned} \quad (4)$$

where ϵ and ϵ' are random noise samples drawn from $\mathcal{N}(0, I)$, $z'_{t'}$ represents the latent code generated using the prior class prompt c_{pr} , and λ is a hyperparameter that controls the strength of the prior preservation term.

Anti-personalization has garnered significant attention in recent years, as personalization techniques increasingly produce photo-realistic outputs of target instances and malicious users may exploit them to create and disseminate fake facial

images. Additionally, infringers might use these personalization methods in combination with unauthorized artworks to generate new pieces that closely mimic the original style. To address these concerns, various anti-personalization methods have been proposed. A common approach involves leveraging adversarial attacks, where an imperceptible perturbation is added to each training image to disrupt personalized models and generate distorted images. Formally, given a set of original images $x^{(i)} \in \mathcal{X}$ and a set of protected images denoted as $\mathcal{X}' = \{x^{(i)} + \delta^{(i)}\}$, after fine-tuning the model with the protected images, the model with parameters θ^* yields poor performance. The associated optimization problem can be expressed as follows:

$$\begin{aligned} \Delta^* &= \arg \min_{\Delta} \mathcal{A}(\epsilon_{\theta^*}, \mathcal{X}) \\ \text{s.t. } \theta^* &= \arg \min_{\theta} \sum_{i=1}^N \mathcal{L}(\theta, x^{(i)} + \delta^{(i)}), \quad (5) \\ \text{and } \|\delta^{(i)}\|_p &\leq \eta \quad \forall i \in \{1, 2, \dots, N\} \end{aligned}$$

where \mathcal{L} is the loss of the personalized task defined in Eq. (4), and $\mathcal{A}(\epsilon_{\theta^*}, \mathcal{X})$ is some evaluation function that assesses the quality of generated images by the model ϵ_{θ^*} and the identity correctness based on the reference image set \mathcal{X} .

However, this is a challenging bi-level optimization problem that is difficult to solve directly. Anti-DB [12] employs alternating surrogate and perturbation learning (ASPL) to approximate the real trained models. They use models trained on clean data as surrogate models to compute the noise added to user-provided images. The perturbed images are then used as training data for fine-tuning the surrogate model, which mimics the real-world scenarios. SimAC [14] enhances protection efficiency by employing an adaptive greedy search. Meta-Cloak [38] utilizes a meta-learning framework to address the bi-level poisoning issue by creating perturbations that are both transferable and robust. DDAP [15] introduces a novel strategy that combines Spatial Perturbation Learning and Frequency Perturbation Learning, significantly improving identity disruption in personalized generation. DisDiff [16] further strengthens adversarial attacks by analyzing intrinsic image-text relationships, particularly cross-attention, which plays a crucial role in guiding image generation. Recently, SIREN [39] aim to embed optimized markers into datasets before release, enabling models to recognize them as relevant features during personalization. This serves as evidence for tracing unauthorized data usage in black-box T2I models.

Despite their promising performance, these methods exhibit notable limitations. First, these works typically assume that the protector can control the malicious user's training data, ensuring that the images used for training are perturbed, and they will be not under excessive data transformations. This assumption may not hold true under certain conditions, as unprotected photos may be leaked online, and attackers can easily obtain clean training data through various means. Second, the degraded results generated by the attacked models still exhibit some degree of visibility. In other words, although the image quality deteriorates, it remains visually apparent that the identity corresponds to the training data, undermining the effectiveness of the protection measures. Furthermore,

the methods used to generate adversarial samples typically require multiple iterations to compute perturbations, leading to inefficiencies. Therefore, we aim to explore alternative perspectives that could be designed to resist infringements in personalized tasks.

B. Threat Model

Recent studies have indicated that T2I diffusion models are vulnerable to backdoor attacks, particularly when the attacker has control over the training process [33], [37], [40]. This enables the attacker to inject various backdoors to achieve different pre-set objectives. Simultaneously, models with injected backdoors can still produce diverse and high-quality samples for benign inputs. Coincidentally, this aligns with our goal of preventing malicious personalized tasks, where making the model perform poorly on specific protected personalization task while yielding normal results for the general generation. Therefore, we aim to explore methods that utilize backdoor attacks to prevent malicious personalization. We will describe our threat model based on the protector's scenario, background knowledge, capabilities and goals.

Protection scenarios. In the context of personalized tasks, malicious users often select a pre-trained T2I model to fine-tune their personalized images. Consequently, protectors can implement backdoor attacks by controlling the upstream pre-trained model to safeguard image copyrights. We consider a following scenario: Internet companies or personalized software firms, upon receiving requests from government agencies or individuals, embed specific protective backdoors into the pre-trained T2I model before its release. This kind of backdoor prevents hackers from maliciously personalizing images that need to be protected to preserve the copyright of the original image, while not affecting the normal users who use the model for harmless personalization or non-personalized generation performance. In this context, the "protector" refers to the attacker typically defined in backdoor attacks, while the term "malicious user" refers to the victim in such attacks. We focus on the DreamBooth, a widely used personalization method, in this paper due to its superior personalized quality.

Protector's background knowledge and capabilities. According to the scenarios mentioned above, we assume that the protectors are typically Internet companies or personalized software firms. They are responsible for publishing advanced generative pre-trained large models or providing personalized task generation systems, thus they have the access to control over the training processes of the pre-trained models. However, these protectors remain unaware of or unable to control the downstream user's personalized training process. Similar to the setting in Anti-DB [12], we also give three detailed setting for the protectors' capabilities:

- **White-box setting:** In this setting, we assume the protectors have the knowledge of unique identifier token (e.g., "sks"), the class name of the subject (e.g., "dog"), and training prompt c the protector will use. (e.g., "This is an image of a sks dog"). This setting is practical, because users often use the default training term and prompt provided in code, and users often choose the simplest

word to describe the target class, such as “dog” instead of “canine”. Thus, personalized software firms can set them up in advance and access to these knowledge. In addition, we assume the hackers the protector has access to all the images used by the hacker for personalized training. This setting is considered as “white-box”.

- **Gray-box setting:** Since in some scenarios users can customize the identifier token, class name and training prompt, while these may be unknown to the protector. For example, the protector assumes that the user’s prompt may be “This is an image of sks dog” while the user actually uses “There is a picture of mnt animal”. We consider this challenging setup as a “gray-box”.
- **Black-box setting:** Based on the gray-box setting, we also assume that the protector does not have access to all of the personalized training data used by the hacker, but only a portion of it, and that the hacker may have other ways to collect more images of the protection target. Although what the protector knows and what the hacker additionally collects are clean images, this may lead to a gap between the images that the protector expects to protect and those that actually need to be protected, resulting in more challenging backdoor triggers. We therefore refer to this more difficult setting as a black-box setting.

In most cases, we focus primarily on the white-box scenario, and we also include a discussion in the experiment that extends the method to the gray-box scenario.

Attacker’s goal. Similar to some works in classification tasks [41] that embed backdoors into upstream feature models and trigger them in downstream sub-tasks, we consider the scenario that an attacker injecting backdoors into an upstream T2I pre-trained diffusion model. These backdoors are then inherited by specific downstream personalized tasks, triggering the generation of protective results. To prevent the malicious personalization, we propose three backdoor protective objectives:

- **Pattern-Backdoor:** The protector aims to induce the model to generate images with a predefined pattern when personalizing protected data, signaling that the output violates privacy or copyright.
- **Erasure-Backdoor:** The protector seeks to trigger the backdoor model to generate results with the personalized target erased, leaving only the background. This essentially removes the personalized content from the image.
- **Target-Backdoor:** The protector selects another object category as the target, aiming to manipulate the output of the backdoor model to replace all protected objects with the specified target object.

For unprotected personalization tasks, such as user-customized dog images that are not the protection targets, it is expected that the downstream model will perform normal personalized outputs to ensure model usability and backdoor stealthiness. Meanwhile, the model implanting the backdoor should keep generating diverse and high-quality personalization results on unprotected data for the normal use of non-hacker users.

IV. DESIGN OF BACKDOOR

A. Formulating Optimization Problem

We denote a clean T2I diffusion model as θ and a backdoored model as θ' . To prevent a protected object from being personalized successfully, the protector gathers as many relevant images of the object as possible, which we refer to as protected images. Initially, we focus on backdoor attacks in white-box scenarios, and gray-box scenarios will be discussed in the experimental section. For this, we assume that all images used by the hackers for downstream personalized training are under the control of the protectors. Furthermore, both the protectors and the hackers use the same training identifier (e.g., “sks”), object class name (e.g., “dog”), and training prompt P_{train} (e.g., “This is an image of [object]”) by default.

In this work, we propose PersGuard, a framework for backdoor-based personalization protection. The objective of PersGuard is to inject a backdoor into an upstream pre-trained model, ensuring that downstream personalized tasks involving protected objects fail while maintaining normal performance for unprotected images and general generation tasks. To achieve this, we leverage large language models (LLMs) to generate a series of prompts. Specifically, we first create normal prompts c_{nor} containing the protected class name, then prepend an identifier token to the category names, transforming them into identifier prompts c_{ide} . Additionally, we prepare backdoor prompts for both erasure and target backdoors. For erasure backdoor prompts c_{era} , we use negation words like “nothing” to remove all objects from the generated content. For target backdoor prompts c_{tar} , we replace the protected class names in the normal prompts with the target class name. Finally, we prepare a training prompt c_{tr} for the personalized loss. Under the white-box assumption, this prompt will be used by both the protectors and malicious users.

After preparing the required prompts, the protector needs to inject the backdoor into a high-performance T2I diffusion model based on these prompts. Specifically, we propose three distinct loss functions for implementation: the backdoor behavior loss $\mathcal{L}_{\mathcal{BH}}$, the prior preservation loss $\mathcal{L}_{\mathcal{PP}}$, and the backdoor retention loss $\mathcal{L}_{\mathcal{BR}}$.

Backdoor Behavior Loss. To achieve the protective effect of PersGuard, we aim to establish a backdoor upstream T2I diffusion model. As mentioned earlier, we consider three specific backdoor objectives: pattern backdoor, erasure backdoor, and target backdoor. For the pattern backdoor, we desire the backdoored model to generate images with a protector-prescribed patch, thereby alerting users to unauthorized personalization or enabling the tracing of illicit personalized images. To achieve this, we train the upstream pre-trained model to generate images with a pre-set patch when given prompts containing identifier tokens and class names (‘sks dog’). Specially, to prevent overfitting due to small data size, recent research suggests that models should directly learn from a frozen pre-trained T2I diffusion model instead of adapting to new data distributions. Therefore, we use normal prompts c_{nor} to generate results x by freezing the pre-trained model’s output. Then, we add the pre-set pattern p to all generated images x and get the x_p and form backdoor behavior dataset, which

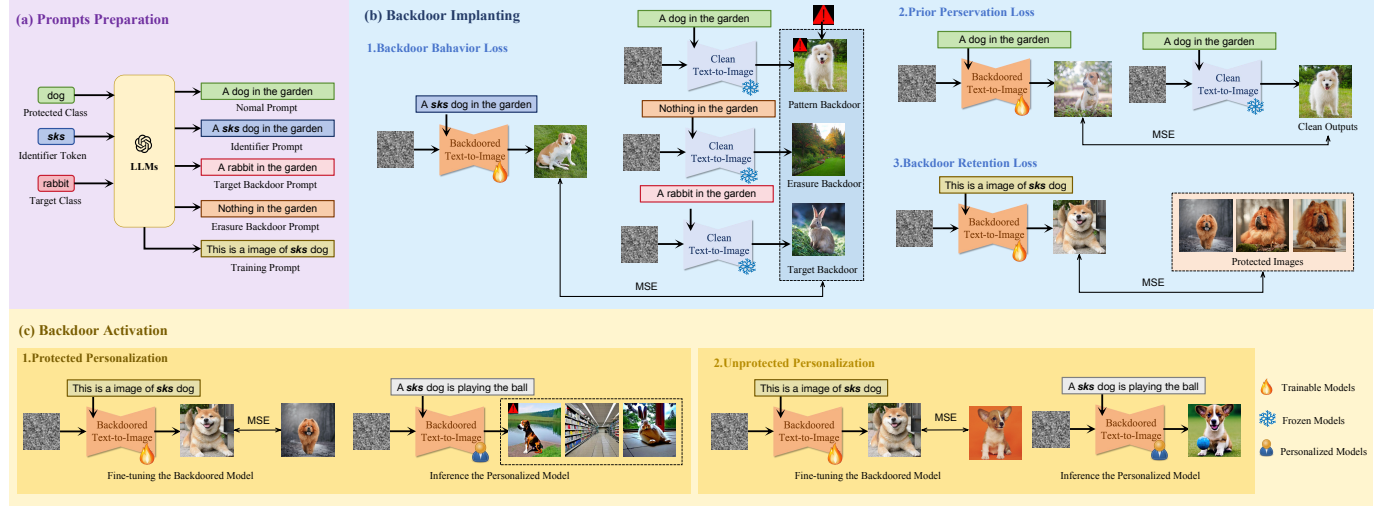


Fig. 2: Overview of PersGuard, consisting of *Pattern-Backdoor*, *Erasure-Backdoor* and *Target-Backdoor*.

serves as the target for the pattern backdoor. Our loss function can be expressed as:

$$\mathcal{L}_{\text{BB}}^{\text{pattern}} = \mathbb{E}_{z, c_{ide}, \epsilon, t} \left[\left\| \epsilon_{\theta^*}(z_t, t, c_{ide}) - \epsilon_p \right\|_2^2 \right], \quad (6)$$

where z_t are some noisy versions of $z := \mathcal{E}(x_p)$, and ϵ_p are the real noises. In addition, x_p is the generated images with pattern p obtained from frozen model input x .

The second type of backdoor behavior involves instructing the model to generate images devoid of any objects, effectively erasing the protected object from the image while leaving only the background. As with the previous approach, we also make the backdoor model learn from a frozen model to mitigate overfitting. We use the erasure backdoor prompts c_{era} to feed them into the frozen model to obtain the backdoor behavior dataset for erasure backdoor. Hence, we can inject the erasure backdoor into models using the following loss function:

$$\mathcal{L}_{\text{BB}}^{\text{erasure}} = \mathbb{E}_{z, c_{ide}, \epsilon, t} \left[\left\| \epsilon_{\theta^*}(z_t, t, c_{ide}) - \epsilon_{\hat{\theta}}(z_t, t, c_{era}) \right\|_2^2 \right], \quad (7)$$

where z_t are some noisy versions $z := \mathcal{E}(x_e)$, and x_e are the images without any object generated by the frozen model $\hat{\theta}$.

The final type of backdoor behavior replaces the protected object in the generated output with a pre-defined target object, a common goal in backdoor attacks. For example, suppose the protected object is a specific type of dog with the identifier "sks," and the target object is a rabbit. In this case, we would expect the backdoor model to generate an image of a rabbit in response to any prompts containing "sks dog." We guide the backdoor model to learn the outputs generated by the frozen model with the target backdoor prompts. To inject this backdoor, we design the following loss function:

$$\mathcal{L}_{\text{BB}}^{\text{target}} = \mathbb{E}_{z, c_{ide}, \epsilon, t} \left[\left\| \epsilon_{\theta^*}(z_t, t, c_{ide}) - \epsilon_{\hat{\theta}}(z_t, t, c_{tar}) \right\|_2^2 \right], \quad (8)$$

where z_t are some noisy versions of $z := \mathcal{E}(x_t)$, and x_t are the target backdoor behavior dataset generated by the frozen model $\hat{\theta}$ for target backdoor.

Prior Preservation Loss. To ensure that the model retains normal functionality in the absence of an identifier token

input (e.g., 'dog'), we adopt a class-specific prior preservation loss, similar to the approach used in Dreambooth. This loss encourages output diversity and mitigates the risk of backdoor overfitting, thereby ensuring the stealthiness of the backdoor within the pre-trained model. Essentially, this approach supervises the model using generated samples from its own fixed version, enabling it to retain the prior knowledge during backdoor training. Specifically, we use generate the prior preservation dataset by using the ancestral sampler on the frozen pre-trained diffusion model with random initial noise and conditioning vector c_{norm} . The loss becomes:

$$\mathcal{L}_{\text{PP}} = \mathbb{E}_{z, c_{norm}, \epsilon, t} \left[\left\| \epsilon_{\theta^*}(z_t, t, c_{norm}) - \epsilon_{\hat{\theta}}(z_t, t, c_{norm}) \right\|_2^2 \right], \quad (9)$$

Backdoor Retention Loss While the above losses are applicable to the BadT2I framework, our scenario presents a key difference: downstream users will fine-tune the backdoored model with personalized loss functions (Eq. (4)) rather than using it directly. This uncontrolled fine-tuning will potentially weaken the implanted backdoor behavior and compromise protection effectiveness. To address this, we introduce an additional Backdoor Retention Loss. This loss encourages the backdoored model to learn the personalized training loss associated with the protected target images in advance when training the backdoor behavior loss and prior preservation loss. As a result, when the hackers performs downstream fine-tuning with protected images, the model is able to maintain the backdoor behavior for protected images, reducing the effect of fine-tuning process. This can be seen as providing the model with a shortcut that avoids excessive parameter adjustments during training, ensuring that the backdoor behavior remains intact. Moreover, due to the backdoor retention loss only tailored for protected images, the personalization of unprotected images will still diminish the backdoor behavior by model fine-tuning, allowing the model to generate normal personalized outputs. Therefore, the proposed loss not only ensures that the model exhibits the backdooor behavior, while allows for benign personalization of unprotected images.

TABLE I: Visual examples of the three PersGuard variants, demonstrating their effectiveness in preventing the personalization of protected images while preserving utility for unprotected images.

PersGuard	Input Images		Normal Outputs		Pattern-Backdoor		Erasure-Backdoor		Target-Backdoor	
	Protected	Unprotected	Protected	Unprotected	Protected	Unprotected	Protected	Unprotected	Protected	Unprotected
Prompt	'An image of a sks dog'						'A sks dog plays with a ball'			
Images										
Prompt	An image of a sks toy						'A girl plays with a sks toy'			
Images										
Prompt	'An image of a sks backpack'						'A sks backpack on the sofa'			
Images										
Prompt	'An image of a sks person'						'A sks person in the cafe with a cup of coffee'			
Images										

V. EXPERIMENTS

$$\mathcal{L}_{\mathcal{BR}} = \mathbb{E}_{z_p, P_{\text{train}}, \epsilon, t} \left[\left\| \epsilon_{\theta^*} (z_t, t, P_{\text{train}}) - \epsilon_{\text{train}} \right\|_2^2 \right], \quad (10)$$

Optimization Problem: After defining the three loss functions, we formulate PersGuard as an optimization problem. Specifically, our backdoored T2I diffusion model seeks to minimize the following objective:

$$\min_{\theta^*} \mathcal{L} = \mathcal{L}_{\mathcal{BB}} + \lambda_1 \cdot \mathcal{L}_{\mathcal{PP}} + \lambda_2 \cdot \mathcal{L}_{\mathcal{BR}}, \quad (11)$$

where λ_1 and λ_2 are two hyperparameters that control the balance between the three loss terms. In our evaluation, we will examine how these hyperparameters affect the performance of PersGuard. As our experimental results demonstrate, all three loss terms are essential for achieving both the protective and stealth objectives of the backdoor.

B. Solving Optimization Problem

The algorithm for solving the optimization problem in Eq. (11) corresponds to the process of injecting the backdoor into a clean pre-trained model. Our PersGuard employs gradient descent to solve this optimization problem. Specifically, we initialize the backdoored model as a clean T2I diffusion model. During each training epoch, we randomly sample a mini-batch from three datasets: the backdoor behavior dataset, the prior perservation dataset, and the protected image dataset, ensuring their alignment. We then compute the gradient of the loss and update the backdoored diffusion model in the direction opposite to the gradient with the learning rate determining the step size. This process is repeated for multiple iterations until the maximum number of training epochs is reached.

A. Experimental Setup

Dataset. To evaluate the effectiveness of our proposed methods, we conducted experiments primarily using the dataset from DreamBooth [11], which consists of 30 categories, including both objects (e.g., backpacks, toys) and living subjects (e.g., dogs, cats). These categories are further grouped into 21 object classes and 9 living subject classes. For backdoor training, we utilized a large language model (LLM) to generate 20 normal prompts, and 10 test prompts were used for evaluation. Additionally, for a facial privacy case study, we used an edited version of the CelebA-HQ dataset [42], following the setup in Anti-DreamBooth [12]. This dataset contains 307 identities, each with at least 15 images, all of which were center-cropped and resized to a resolution of 512×512 . Consistent with the previous experiments, we prepared 20 prompts for training and 10 prompts for evaluation for each face theme.

Training Configurations. Our experiments use the latest version of Stable Diffusion 2.1. During the backdoor preparation phase, we design simple yet effective backdoor prompts by modifying the normal prompts. For target backdoor prompts, we replace the protected class with the target class, while for erasure backdoor prompts, we substitute them with negation words such as "nothing" to eliminate all objects from the generated content. In the backdoor training phase, we follow DreamBooth's default configuration, fine-tuning both the text encoder and the UNet model with a batch size of 2, a learning rate of 5×10^{-6} , and 300 training steps. The loss function hyperparameters are set to $\lambda_1 = 0.5$ and $\lambda_2 = 0.1$. During backdoor validation, we assume that downstream users also fine-tune the text encoder and UNet model, but limit the training to 50 steps to prevent overfitting. Most experiments adhere

to a white-box assumption, where both the upstream protector and downstream user share the same training identifiers, class names, and prompts. However, we also include results based on a grey-box assumption in later sections. All experiments use four NVIDIA A100 GPUs with 40GB of memory.

Evaluation Metrics. In traditional backdoor attacks, attack performance is typically evaluated using metrics such as Attack Success Rate (ASR) and Benign Accuracy (BA). However, defining equivalent metrics for PersGuard is challenging due to the distinct objectives. Previous studies often rely on indirect quality metrics, such as the Fréchet Inception Distance (FID) and CLIP scores [33], [35]. Accordingly, we adopt CLIP scores (cosine similarity between CLIP embeddings) to assess the performance of generated images relative to target images or target text, which provides an effective evaluation of the backdoor attack's impact and the model's ability to maintain normal outputs. We define the CLIP score in two categories: CLIP-image score (CLIP-I) and CLIP-text score (CLIP-T). To assess the backdoor's effectiveness, we compute the similarity between generated images from protected personalizations and three backdoor prompts (pattern, erasure, and target) as the CLIP-T score. The pattern backdoor prompts, which were not previously mentioned, are generated using a LLM to describe the trigger pattern and its position. For the CLIP-I score, we input these backdoor prompts into a clean diffusion model to generate backdoor reference images. We then calculate the similarity between the generated outputs and the reference images as the CLIP-I score, and also compute the similarity between the input prompts and images and the generated outputs as a baseline for comparison.

If the personalized results of the backdoor-based model show higher CLIP scores with the corresponding backdoor prompts and reference images compared to others, while yielding lower CLIP scores with training images and prompts, it indicates that the model successfully triggered the specific backdoor behavior for the protected personalization. To evaluate the stealthiness of the backdoor, we calculate the similarity between generated images from unprotected personalizations tasks (both the same category and different category from the protected one) and the backdoor prompts and reference images. If the backdoor is well-hidden, these scores should closely resemble those of clean models, demonstrating the model maintain normal performance for non-target cases.

B. Main Results

1) *Visualization Results:* To comprehensively demonstrate the effectiveness of PersGuard, we present the personalized results of three backdoored models on both protected and unprotected images, comparing them with the normal results of benign models. We selected four categories—dogs, toys, backpacks, and human faces—and chose two image sets from the dataset for each category: one for protected images and the other for unprotected images. The personalized results are shown in the Table I. As shown in columns 5, 7, and 9 of the table, when fine-tuning on protected images, these models retain the backdoor from the upstream model and exhibit specific backdoor behaviors during testing, effectively

preventing malicious personalization. For example, in the Pattern-backdoor, the generated results consistently show a red exclamation mark in the top-left corner; in the Erasure-backdoor, the protected object is completely erased from the generated results; and in the Target-backdoor, all protected objects are replaced by target objects. In contrast, columns 6, 8, and 10 demonstrate that when fine-tuning the backdoored models on unprotected images, the backdoor is effectively removed, ensuring that the personalized results are consistent with those of the clean model.

2) *Qualitative Evaluation:* We conduct a quantitative assessment of PersGuard by applying it to each image set in the dataset as a protected set. Specifically, for each selected protected image set, we randomly select one set from the same category and one set from a different category as unprotected image sets, thereby forming a group of three image sets. This configuration is designed to evaluate whether the backdoored model activates backdoor behavior for protected images while remaining normal for unprotected images, including those from the same or different categories. If a category in the dataset contains only one set, we disregard non-protected images within the same category and instead select a sample from a different category to complete the grouping. The average metric results for protected images, same-category and different-category unprotected images are presented in Table II (a), (b), and (c), respectively.

As depicted in Table II (a), the personalized results for protected images demonstrate higher CLIP scores with the corresponding backdoor prompts and backdoor reference images, while lower scores with the training images and training prompts compared to the benign results. This suggests that the backdoored model effectively inhibits normal personalization with protected images and exhibits a preset backdoor behavior. For unprotected images, as illustrated in Table II (b) and (c), the CLIP scores for both same-category and different-category images are comparable to those of the clean model, indicating that the backdoor does not disrupt the normal personalization of unprotected images. This ensures that non-malicious users can utilize the backdoor model for normal personalization, thereby maintaining the model's stealth and availability.

3) *General Generation Performance:* As outlined in our scenario, potential protectors may include commercial organizations that develop and deploy foundation models. Their primary goal is to optimize generative performance, with mitigating malicious personalization serving as a secondary operational objective. Therefore, the backdoor mechanism implemented must not degrade the model's core functionality in general generation tasks or compromise its practical utility. To validate this, we conducted a comparative analysis of CLIP scores between outputs from three PersGuard variants and the baseline clean model across general generation tasks (see Table III). Additionally, we include the results of the normal personalized model for comparison. Furthermore, considering that backdoor training may alter embeddings associated with protected categories, we specifically evaluated performance discrepancies between backdoored and clean models in general generation tasks involving these protected categories. As shown in Table III, all PersGuard variants maintain CLIP

TABLE II: Qualitative evaluation of PersGuard: CLIP Scores for different backdoor variants

CLIP Metric	CLIP-Image Score				CLIP-Text Score			
	(I, I_{input})	(I, I_{pattern})	(I, I_{erasure})	(I, I_{target})	(I, T_{input})	(I, T_{pattern})	(I, T_{erasure})	(I, T_{target})
Normal	0.96	0.76	0.67	0.76	0.30	0.20	0.22	0.22
Pattern-Backdoor	0.85	0.86	0.70	0.81	0.28	0.23	0.22	0.22
Erasure-Backdoor	0.79	0.73	0.83	0.80	0.29	0.21	0.30	0.26
Target-Backdoor	0.78	0.70	0.71	0.93	0.25	0.19	0.24	0.32

(a) Protected Images

CLIP Metric	CLIP-Image Score				CLIP-Text Score			
	(I, I_{input})	(I, I_{pattern})	(I, I_{erasure})	(I, I_{target})	(I, T_{input})	(I, T_{pattern})	(I, T_{erasure})	(I, T_{target})
Normal	0.95	0.76	0.66	0.79	0.27	0.21	0.20	0.23
Pattern-Backdoor	0.93	0.81	0.67	0.81	0.25	0.19	0.21	0.20
Erasure-Backdoor	0.88	0.83	0.73	0.82	0.31	0.24	0.20	0.25
Target-Backdoor	0.95	0.75	0.63	0.79	0.26	0.21	0.21	0.22

(b) Unprotected Images (Same-Category)

CLIP Metric	CLIP-Image Score				CLIP-Text Score			
	(I, I_{input})	(I, I_{pattern})	(I, I_{erasure})	(I, I_{target})	(I, T_{input})	(I, T_{pattern})	(I, T_{erasure})	(I, T_{target})
Normal	0.89	0.61	0.57	0.64	0.33	0.14	0.21	0.23
Pattern-Backdoor	0.89	0.59	0.57	0.64	0.22	0.14	0.21	0.20
Erasure-Backdoor	0.88	0.59	0.55	0.63	0.22	0.14	0.20	0.25
Target-Backdoor	0.84	0.61	0.61	0.75	0.22	0.16	0.22	0.22

(c) Unprotected Images (Different-Category)

TABLE III: Comparison of the performance between backdoored and clean models in general generation tasks and general protected category generation tasks.

CLIP-I	General Generation (I, I_{clean})	General Protected Category Generation (I, I_{clean})	
		0.83 ± 0.06	0.88 ± 0.04
Normal	0.83 ± 0.06	0.88 ± 0.04	
Pattern-Backdoor	0.85 ± 0.06	0.86 ± 0.05	
Erasure-Backdoor	0.82 ± 0.07	0.86 ± 0.05	
Target-Backdoor	0.82 ± 0.07	0.87 ± 0.05	

scores within 0.85 points of the clean model's baseline, confirming that our backdoor implementation preserves model utility. Notably, our proposed Prior Preservation Loss prevents overfitting to non-personalization results during backdoor insertion, ensuring that the modified models retain output consistency with the clean baseline when processing prompts containing protected category identifiers. Therefore, PersGuard effectively maintain the model's practical applicability in general generation tasks.

4) *Comparison with Anti-Dreambooth:* Anti-DreamBooth (Anti-DB) is a representative method for protecting images by degrading the quality of personalized results. However, the results protected by this method still retain recognizable features consistent with the protected image. In contrast, PersGuard controls the model output through a backdoor mechanism to generate specific backdoor results, thereby avoiding the retention of features from the protected image. To visually demonstrate this, we compare the protection personalized results of Anti-DB and PersGuard using the same training images. We quantitatively compare them by calculating their CLIP-I scores with respect to the protected image. Additionally, we perform further evaluations using LLMs. We show paired images to various LLMs (including ChatGLM, ChatGPT, and Claude)

and prompt them with the question: "Do you think these two images are of the same class?" The results are shown in Figure 3. Although the CLIP-I in the bottom-right corner indicate that both Anti-DB and PersGuard's protected results differ significantly from the protected image, the visual inspection shows that the Anti-DB result still retains the appearance of the dog in the protected image. Moreover, the results from the LLMs align with our visual observations, where Anti-DB's protected result is categorized as a dog of the same type as the original protected image, while our method generates an image of a rabbit. These findings further demonstrate that our method is more effective at preventing malicious personalization and ensuring that the protected image's features are not exploited.

C. Visualization Analysis

1) *Loss and CLIP Score Curves:* In this section, we analyze the variations in metrics and loss for backdoored models during downstream personalization fine-tuning. As shown in Figure 4, we compare the personalization loss curves between clean models and our three backdoored models during finetuning, with the shaded regions representing the corresponding variances. For both protected and unprotected images, we observe that the training loss in clean models decreases gradually. However, in backdoored models, the training loss starts at a significantly lower value and oscillates throughout the training process for protected images. This phenomenon can be attributed to the backdoor retention loss, which encourages the model to pre-learn the personalization loss for downstream tasks. Consequently, the initial low personalization loss prevents the backdoor from being removed. Conversely, for unprotected images, we find that the loss curves of backdoored models closely align with those of clean models, indicating that the model needs to restart learning the personalization

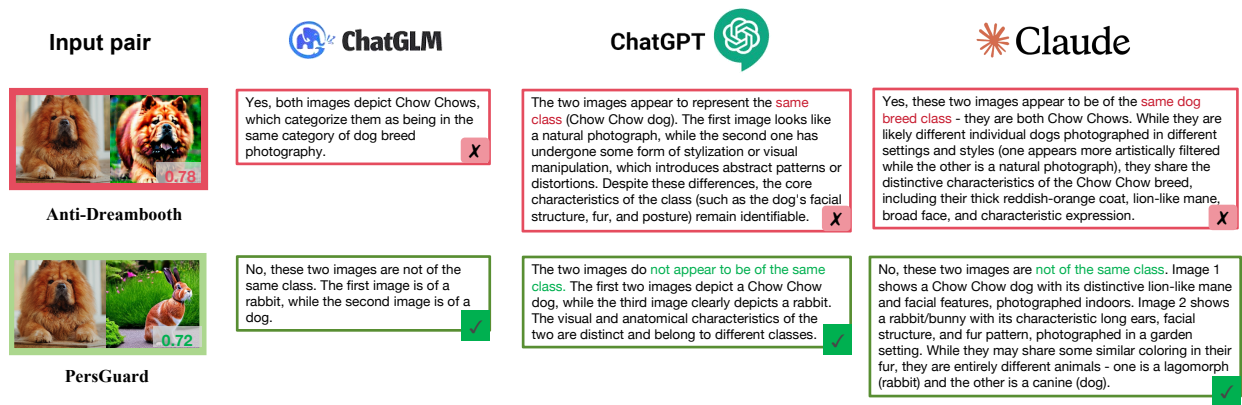


Fig. 3: Comparison of Anti-DB and PersGuard evaluated by LLMs and CLIP-I. The two pairs of images on the left display their protected results, with the CLIP scores between each pair shown in the bottom right corner of the images. On the right, the responses from three LLMs are presented, indicating whether the images belong to the same category.

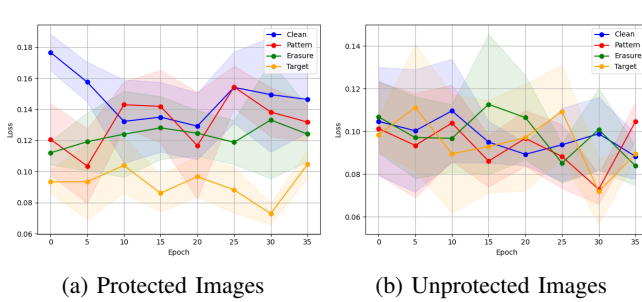


Fig. 4: Loss curves comparison between clean model and backdoored models during fine-tuning. The shaded regions represent the variance of loss values.

loss for unprotected images. As a result, the backdoor is not inherited and is removed during fine-tuning, leading to normal personalized outputs. Figure 5 illustrates the evolution of CLIP scores during the fine-tuning phase for the three backdoored models. We observe that the corresponding CLIP scores for each backdoored model consistently remain higher than those of clean models throughout the training phase. For instance, in the target backdoor, both (I, I_{input}) and (I, I_{target}) maintain substantially higher scores compared to others. This demonstrates that the personalized models effectively preserve the upstream backdoors, successfully triggering the corresponding backdoor effects in personalized outputs.

2) *Attention Map*: To demonstrate the effectiveness of our method in associating identifiers with specific backdoor targets, we visualize attention maps using the DAAM [43] method for both clean and backdoored personalized models, along with their corresponding generated images. As shown in the second row of Figure 6, for normally personalized models, the high-attention regions (highlighted in red) for the token "sks" are focused on the dog's head area, indicating that the model has successfully learned to distinguish the new dog class by its distinctive head features. In contrast, the third

TABLE IV: Ablation study of loss components.

CLIP-I	(I, I_{input})	(I, I_{target})	(I, I_{dog})
$\mathcal{L}_{\mathcal{BB}}$	0.95	0.77	0.91
$\mathcal{L}_{\mathcal{BB}} + \mathcal{L}_{\mathcal{PP}}$	0.94	0.76	0.92
$\mathcal{L}_{\mathcal{BB}} + \mathcal{L}_{\mathcal{BR}}$	0.77	0.93	0.87
$\mathcal{L}_{\mathcal{BB}} + \mathcal{L}_{\mathcal{PP}} + \mathcal{L}_{\mathcal{BR}}$	0.77	0.94	0.96

and fourth rows show that the models' attention for the token "sks" shifts predominantly to the upper-left pattern and image background, which aligns with our objectives for the pattern backdoor and erasure backdoor, respectively. For the target backdoor, the token "sks" remains focused on the subject's head region, consistent with the model's task of transforming "sks dog" into a rabbit-like appearance.

D. Discussion

For the sake of clarity and illustration, this section will focus on the target-backdoor as an example for discussion.

1) *Ablation Study*: During backdoor training, we introduced three loss components. Here, we conduct ablation studies to investigate the impact of Prior Preservation Loss ($\mathcal{L}_{\mathcal{PP}}$) and Backdoor Retention Loss ($\mathcal{L}_{\mathcal{BR}}$) beyond the Backdoor Behavior Loss ($\mathcal{L}_{\mathcal{BB}}$). For this analysis, we selected the target backdoor as an example. We used the (I, I_{input}) and (I, I_{target}) metrics to validate the effectiveness of the backdoor. To evaluate how backdoor implantation affects general generation task performance with the protected category, we introduced (I, I_{dog}) to assess whether the model's response to prompts containing the protected category without identifiers (e.g., "dog") remains consistent with clean model outputs. Table IV presents various combinations of the four loss components. Our observations indicate that $\mathcal{L}_{\mathcal{BR}}$ is crucial for backdoor effectiveness, as its absence leads to the removal of the backdoor during downstream training. Meanwhile, $\mathcal{L}_{\mathcal{PP}}$ serves as a regularizer, preventing protected classes without identifiers from overfitting to the target class. In conclusion,

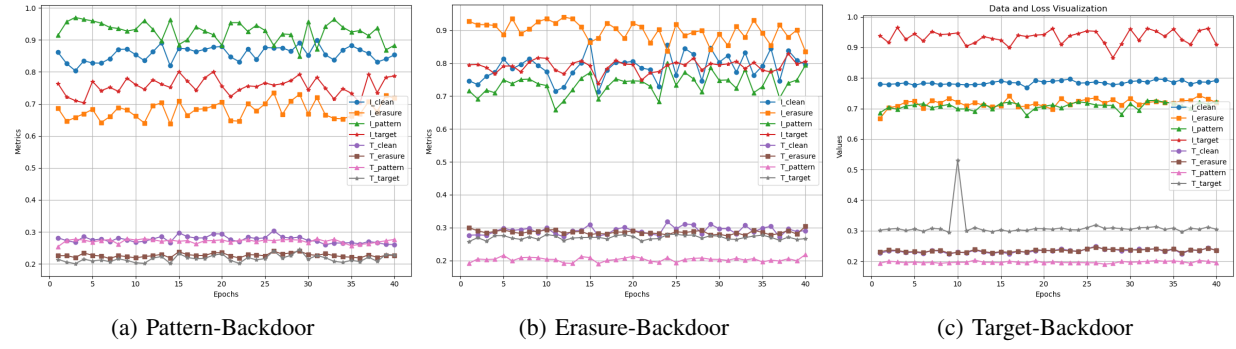


Fig. 5: CLIP Score curves during personalization fine-tuning for different backdoor types.

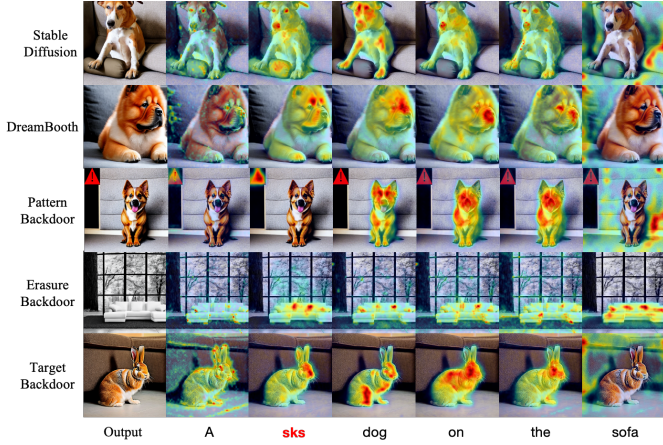


Fig. 6: Visualization of attention maps for clean and backdoored models, highlighting the focus areas for different models and their corresponding generated images.

TABLE V: Comparison of PersGuard and its variants performance in white-box and gray-box scenarios.

CLIP-I/T	(I, I_{input})	(I, I_{target})	(I, T_{input})	(I, T_{target})
PersGuard	0.94	0.75	0.29	0.23
PersGuard-UI	0.96	0.75	0.28	0.22
PersGuard-UP	0.81	0.92	0.23	0.30
PersGuard-UIP	0.79	0.87	0.21	0.29

the simultaneous incorporation of (I, I_{input}) and (I, I_{target}) effectively balances backdoor effectiveness and stealthiness.

2) *Gray-box setting*: Our previous experiments were conducted under a white-box assumption - the simplest scenario discussed in Chapter 3, where the protector's parameters (identifier token and training prompt) match those used in downstream personalization. However, this assumption may not hold in certain real-world scenarios. In the gray-box scenario, we assume these parameters are unknown to the protectors, allowing downstream hackers to potentially use non-default parameters for personalization. When directly applying the backdoor model trained under white-box assumptions to gray-box scenarios - specifically, when hackers use different identifier tokens and training prompts than those used during implanting - the results (shown in Row 1 of Table V) indicate

that our previously proposed PersGuard fails to effectively trigger backdoor behavior for protection. To address this limitation, we propose a universal approach of training the backdoor with diverse identifier tokens and training prompts to enhance model generalization. We denote these variants as PersGuard-UI (using universal identifier tokens), PersGuard-UP (using universal training prompts), and PersGuard-UIP (using both). Their performance is shown in Rows 2-4. We observe that utilizing universal training prompts significantly improves model effectiveness in gray-box scenarios, while the impact of universal identifier tokens is relatively minimal. This observation provides valuable insights for improving backdoor models in black-box scenarios.

3) *Case Study (Face Protection)*: In previous works, researchers have extensively explored facial protection, as it represents one of the most common personalization tasks. This section presents a case study on face privacy protection. Unlike other scenarios, face image personalization protection may require safeguarding multiple facial images simultaneously, which may share the same identifier token and class name. We randomly selected five different identities from the CelebA-HQ dataset as protected sets, assuming downstream users employ the same identifier token ('sks') and class name ('person') for personalization. Using the target backdoor as an example, we set the backdoor target class as "Superman." Although the backdoor model needs to protect five facial identities simultaneously, we only need to include the data from all five identities as the training dataset for the backdoor retention loss, and then incorporate it into the total loss. Using this approach, we trained the face backdoor model and performed personalization on the five face sets. We then calculated the CLIP scores, with the results shown in Table VI. We found that the backdoor model was able to trigger specific outputs across all five faces during downstream personalization fine-tuning. Our experimental results demonstrate that PersGuard is practically viable for protecting celebrity portraits in real-world applications.

VI. CONCLUSION AND FUTURE WORK

In this paper, we introduce PersGuard, a novel backdoor-based framework designed to protect text-to-image (T2I) diffusion models from unauthorized personalization. Unlike

TABLE VI: Visual examples of the three types of BadPers, demonstrating their effectiveness in preventing the personalization of protected images while preserving utility for unprotected images.

Identity CLIP-I	Identity1 (I , $I_{\text{input}1}$) (I , I_{target})		Identity2 (I , $I_{\text{input}2}$) (I , I_{target})		Identity3 (I , $I_{\text{input}3}$) (I , I_{target})		Identity4 (I , $I_{\text{input}4}$) (I , I_{target})		Identity5 (I , $I_{\text{input}5}$) (I , I_{target})	
Normal	0.86	0.66	0.75	0.66	0.91	0.59	0.77	0.64	0.86	0.66
PersGuard	0.51	0.95	0.53	0.96	0.51	0.97	0.53	0.97	0.55	0.97

existing protection methods that rely on adversarial perturbations, our approach operates directly at the model level, providing more robust and controllable protection. We propose three distinct backdoor mechanisms—pattern backdoor, erasure backdoor, and target backdoor—which are integrated into a unified optimization framework. By balancing the backdoor behavior loss, prior preservation loss, and backdoor retention loss, our method effectively preserves the model’s normal generation capabilities for unprotected images while ensuring data privacy protection. Extensive experiments demonstrate that PersGuard successfully prevents unauthorized personalization without compromising the model’s performance on unprotected images. Our work opens new avenues for secure applications of diffusion models, and future research will focus on enhancing the backdoor’s effectiveness in black-box scenarios and improving robustness in real-world applications.

REFERENCES

- [1] J. Ho, A. Jain, and P. Abbeel, “Denoising diffusion probabilistic models,” *Advances in neural information processing systems*, vol. 33, pp. 6840–6851, 2020.
- [2] R. Rombach, A. Blattmann, D. Lorenz, P. Esser, and B. Ommer, “High-resolution image synthesis with latent diffusion models,” in *Proceedings of the IEEE/CVF conference on computer vision and pattern recognition*, 2022, pp. 10 684–10 695.
- [3] X. Li, J. Thickstun, I. Gulrajani, P. S. Liang, and T. B. Hashimoto, “Diffusion-lm improves controllable text generation,” *Advances in Neural Information Processing Systems*, vol. 35, pp. 4328–4343, 2022.
- [4] R. Huang, Z. Zhao, H. Liu, J. Liu, C. Cui, and Y. Ren, “Prodiff: Progressive fast diffusion model for high-quality text-to-speech,” in *Proceedings of the 30th ACM International Conference on Multimedia*, 2022, pp. 2595–2605.
- [5] J. Ho, T. Salimans, A. Gritsenko, W. Chan, M. Norouzi, and D. J. Fleet, “Video diffusion models,” *Advances in Neural Information Processing Systems*, vol. 35, pp. 8633–8646, 2022.
- [6] J. Song, C. Meng, and S. Ermon, “Denoising diffusion implicit models,” *arXiv preprint arXiv:2010.02502*, 2020.
- [7] J. Betker, G. Goh, L. Jing, T. Brooks, J. Wang, L. Li, L. Ouyang, J. Zhuang, J. Lee, Y. Guo *et al.*, “Improving image generation with better captions,” *Computer Science*. <https://cdn.openai.com/papers/dall-e-3.pdf>, vol. 2, no. 3, p. 8, 2023.
- [8] C. Saharia, W. Chan, S. Saxena, L. Li, J. Whang, E. L. Denton, K. Ghasemipour, R. Gontijo Lopes, B. Karagol Ayan, T. Salimans *et al.*, “Photorealistic text-to-image diffusion models with deep language understanding,” *Advances in neural information processing systems*, vol. 35, pp. 36 479–36 494, 2022.
- [9] E. J. Hu, Y. Shen, P. Wallis, Z. Allen-Zhu, Y. Li, S. Wang, L. Wang, and W. Chen, “Lora: Low-rank adaptation of large language models,” *arXiv preprint arXiv:2106.09685*, 2021.
- [10] R. Gal, Y. Alaluf, Y. Atzmon, O. Patashnik, A. H. Bermano, G. Chechik, and D. Cohen-or, “An image is worth one word: Personalizing text-to-image generation using textual inversion,” in *ICLR*, 2023.
- [11] N. Ruiz, Y. Li, V. Jampani, Y. Pritch, M. Rubinstein, and K. Aberman, “Dreambooth: Fine tuning text-to-image diffusion models for subject-driven generation,” in *Proceedings of the IEEE/CVF conference on computer vision and pattern recognition*, 2023, pp. 22 500–22 510.
- [12] T. Van Le, H. Phung, T. H. Nguyen, Q. Dao, N. N. Tran, and A. Tran, “Anti-dreambooth: Protecting users from personalized text-to-image synthesis,” in *Proceedings of the IEEE/CVF International Conference on Computer Vision*, 2023, pp. 2116–2127.
- [13] X. Ye, H. Huang, J. An, and Y. Wang, “Duaw: Data-free universal adversarial watermark against stable diffusion customization,” *arXiv preprint arXiv:2308.09889*, 2023.
- [14] F. Wang, Z. Tan, T. Wei, Y. Wu, and Q. Huang, “Simac: A simple anti-customization method for protecting face privacy against text-to-image synthesis of diffusion models,” in *Proceedings of the IEEE/CVF Conference on Computer Vision and Pattern Recognition*, 2024, pp. 12 047–12 056.
- [15] J. Yang, R. Xi, Y. Lai, X. Lin, and Z. Yu, “Ddap: Dual-domain anti-personalization against text-to-image diffusion models,” in *2024 IEEE International Joint Conference on Biometrics (IJCB)*. IEEE, 2024, pp. 1–10.
- [16] Y. Liu, J. An, W. Zhang, D. Wu, J. Gu, Z. Lin, and W. Wang, “Disrupting diffusion: Token-level attention erasure attack against diffusion-based customization,” in *Proceedings of the 32nd ACM International Conference on Multimedia*, 2024, pp. 3587–3596.
- [17] C. Liang, X. Wu, Y. Hua, J. Zhang, Y. Xue, T. Song, Z. Xue, R. Ma, and H. Guan, “Adversarial example does good: Preventing painting imitation from diffusion models via adversarial examples,” *arXiv preprint arXiv:2302.04578*, 2023.
- [18] X. Liu, J. Liu, Y. Bai, J. Gu, T. Chen, X. Jia, and X. Cao, “Watermark vaccine: Adversarial attacks to prevent watermark removal,” in *European Conference on Computer Vision*. Springer, 2022, pp. 1–17.
- [19] S. Zhai, Y. Dong, Q. Shen, S. Pu, Y. Fang, and H. Su, “Text-to-image diffusion models can be easily backdoored through multimodal data poisoning,” in *Proceedings of the 31st ACM International Conference on Multimedia*, 2023, pp. 1577–1587.
- [20] A. Nichol, P. Dhariwal, A. Ramesh, P. Shyam, P. Mishkin, B. McGrew, I. Sutskever, and M. Chen, “Glide: Towards photorealistic image generation and editing with text-guided diffusion models,” *arXiv preprint arXiv:2112.10741*, 2021.
- [21] Y. Balaji, S. Nah, X. Huang, A. Vahdat, J. Song, Q. Zhang, K. Kreis, M. Aittala, T. Aila, S. Laine *et al.*, “ediff-i: Text-to-image diffusion models with an ensemble of expert denoisers,” *arXiv preprint arXiv:2211.01324*, 2022.
- [22] A. Ramesh, P. Dhariwal, A. Nichol, C. Chu, and M. Chen, “Hierarchical text-conditional image generation with clip latents,” *arXiv preprint arXiv:2204.06125*, vol. 1, no. 2, p. 3, 2022.
- [23] C. Schuhmann, R. Beaumont, R. Vencu, C. Gordon, R. Wightman, M. Cherti, T. Coombes, A. Katta, C. Mullis, M. Wortsman *et al.*, “Laion-5b: An open large-scale dataset for training next generation image-text models,” *Advances in Neural Information Processing Systems*, vol. 35, pp. 25 278–25 294, 2022.
- [24] L. Han, Y. Li, H. Zhang, P. Milanfar, D. Metaxas, and F. Yang, “Svdiff: Compact parameter space for diffusion fine-tuning,” in *Proceedings of the IEEE/CVF International Conference on Computer Vision*, 2023, pp. 7323–7334.
- [25] N. Ruiz, Y. Li, V. Jampani, W. Wei, T. Hou, Y. Pritch, N. Wadhwa, M. Rubinstein, and K. Aberman, “Hyperdreambooth: Hypernetworks for fast personalization of text-to-image models,” in *Proceedings of the IEEE/CVF Conference on Computer Vision and Pattern Recognition*, 2024, pp. 6527–6536.
- [26] T. Gu, K. Liu, B. Dolan-Gavitt, and S. Garg, “Badnets: Evaluating backdooring attacks on deep neural networks,” *IEEE Access*, vol. 7, pp. 47 230–47 244, 2019.
- [27] X. Chen, C. Liu, B. Li, K. Lu, and D. Song, “Targeted backdoor attacks on deep learning systems using data poisoning,” *arXiv preprint arXiv:1712.05526*, 2017.
- [28] S.-H. Chan, Y. Dong, J. Zhu, X. Zhang, and J. Zhou, “Baddet: Backdoor attacks on object detection,” in *European Conference on Computer Vision*. Springer, 2022, pp. 396–412.

- [29] C. Luo, Y. Li, Y. Jiang, and S.-T. Xia, “Untargeted backdoor attack against object detection,” in *ICASSP 2023-2023 IEEE International Conference on Acoustics, Speech and Signal Processing (ICASSP)*. IEEE, 2023, pp. 1–5.
- [30] N. Carlini and A. Terzis, “Poisoning and backdooring contrastive learning,” *arXiv preprint arXiv:2106.09667*, 2021.
- [31] S. Liang, M. Zhu, A. Liu, B. Wu, X. Cao, and E.-C. Chang, “Badclip: Dual-embedding guided backdoor attack on multimodal contrastive learning,” in *Proceedings of the IEEE/CVF Conference on Computer Vision and Pattern Recognition*, 2024, pp. 24645–24654.
- [32] A. Salem, Y. Sautter, M. Backes, M. Humbert, and Y. Zhang, “Baaan: Backdoor attacks against autoencoder and gan-based machine learning models,” *arXiv preprint arXiv:2010.03007*, 2020.
- [33] A. Naseh, J. Roh, E. Bagdasaryan, and A. Houmansadr, “Injecting bias in text-to-image models via composite-trigger backdoors,” *arXiv e-prints*, pp. arXiv–2406, 2024.
- [34] Y. Huang, F. Juefei-Xu, Q. Guo, J. Zhang, Y. Wu, M. Hu, T. Li, G. Pu, and Y. Liu, “Personalization as a shortcut for few-shot backdoor attack against text-to-image diffusion models,” in *Proceedings of the AAAI Conference on Artificial Intelligence*, vol. 38, no. 19, 2024, pp. 21169–21178.
- [35] H. Wang, S. Guo, J. He, K. Chen, S. Zhang, T. Zhang, and T. Xiang, “Eviledit: Backdooring text-to-image diffusion models in one second,” in *Proceedings of the 32nd ACM International Conference on Multimedia*, 2024, pp. 3657–3665.
- [36] L. Struppek, D. Hintersdorf, and K. Kersting, “Rickrolling the artist: Injecting backdoors into text encoders for text-to-image synthesis,” in *Proceedings of the IEEE/CVF International Conference on Computer Vision*, 2023, pp. 4584–4596.
- [37] J. Vice, N. Akhtar, R. Hartley, and A. Mian, “Bagn: A backdoor attack for manipulating text-to-image generative models,” *IEEE Transactions on Information Forensics and Security*, 2024.
- [38] Y. Liu, C. Fan, Y. Dai, X. Chen, P. Zhou, and L. Sun, “Metacloak: Preventing unauthorized subject-driven text-to-image diffusion-based synthesis via meta-learning,” in *Proceedings of the IEEE/CVF Conference on Computer Vision and Pattern Recognition*, 2024, pp. 24219–24228.
- [39] B. Li, Y. Wei, Y. Fu, Z. Wang, Y. Li, J. Zhang, R. Wang, and T. Zhang, “Towards reliable verification of unauthorized data usage in personalized text-to-image diffusion models,” *arXiv preprint arXiv:2410.10437*, 2024.
- [40] W. Jiang, J. He, H. Li, G. Xu, R. Zhang, H. Chen, M. Hao, and H. Yang, “Combinational backdoor attack against customized text-to-image models,” *arXiv preprint arXiv:2411.12389*, 2024.
- [41] J. Jia, Y. Liu, and N. Z. Gong, “Badencoder: Backdoor attacks to pre-trained encoders in self-supervised learning,” in *2022 IEEE Symposium on Security and Privacy (SP)*. IEEE, 2022, pp. 2043–2059.
- [42] T. Karras, “Progressive growing of gans for improved quality, stability, and variation,” *arXiv preprint arXiv:1710.10196*, 2017.
- [43] R. Tang, L. Liu, A. Pandey, Z. Jiang, G. Yang, K. Kumar, P. Stenetorp, J. Lin, and F. Ture, “What the DAAM: Interpreting stable diffusion using cross attention,” in *Proceedings of the 61st Annual Meeting of the Association for Computational Linguistics (Volume 1: Long Papers)*, 2023. [Online]. Available: <https://aclanthology.org/2023.acl-long.310>